Applied and Environmental Microbiology, Nov. 2011, p. 7586–7594 Vol. 77, No. 21
0099-2240/11/$12.00 doi:10.1128/AEM.00465-11

The RNA Polymerase Omega Factor RpoZ Is Regulated by PhoP and Has an Important Role in Antibiotic Biosynthesis and Morphological Differentiation in *Streptomyces coelicolor*▽†

Fernando Santos-Beneit,[1] Mónica Barriuso-Iglesias,[2] Lorena T. Fernández-Martínez,[1] Miriam Martínez-Castro,[2] Alberto Sola-Landa,[1] Antonio Rodríguez-García,[1,2] and Juan F. Martín[1,2]*

Institute of Biotechnology, Avda. Real 1, 24006 León, Spain,[1] and Area of Microbiology, Faculty of Biology and Environmental Sciences, University of León, Campus de Vegazana s/n, 24071 León, Spain[2]

Received 1 March 2011/Accepted 1 August 2011

The RNA polymerase (RNAP) omega factor (ω) forms a complex with the $\alpha_2\beta\beta'$ core of this enzyme in bacteria. We have characterized the *rpoZ* gene of *Streptomyces coelicolor*, which encodes a small protein (90 amino acids) identified as the omega factor. Deletion of the *rpoZ* gene resulted in strains with a slightly reduced growth rate, although they were still able to sporulate. The biosynthesis of actinorhodin and, particularly, that of undecylprodigiosin were drastically reduced in the Δ*rpoZ* strain, suggesting that expression of these secondary metabolite biosynthetic genes is dependent upon the presence of RpoZ in the RNAP complex. Complementation of the Δ*rpoZ* mutant with the wild-type *rpoZ* allele restored both phenotype and antibiotic production. Interestingly, the *rpoZ* gene contains a PHO box in its promoter region. DNA binding assays showed that the phosphate response regulator PhoP binds to such a region. Since luciferase reporter studies showed that *rpoZ* promoter activity was increased in a Δ*phoP* background, it can be concluded that *rpoZ* is controlled negatively by PhoP, thus connecting phosphate depletion regulation with antibiotic production and morphological differentiation in *Streptomyces*.

In bacteria, the RNA polymerase (RNAP) complex plays a central role in transcription and is a target for regulation of primary metabolism (6, 7, 44). The *rpoZ* gene encodes the RNAP omega (ω) subunit, which forms a complex with the $\alpha_2\beta\beta'$ core of this enzyme. The ω subunit has been identified in the RNAPs of most free-living bacteria. This protein is functionally homologous to the RpoK subunit of the archaeal RNA polymerase complex and the RPB6 subunit of the eukaryotic RNA polymerases I, II, and III (32). In *Escherichia coli* the ω subunit interacts with the β′ subunit and promotes assembly of the RNA polymerase complex (14, 32), although it is not essential for survival in this bacterium (13).

Streptomyces spp. are soil-dwelling bacteria that are notorious for their ability to produce thousands of antibiotics, pigments, antitumor agents, immunomodulators, and a variety of other bioactive secondary metabolites (1, 2, 8). Differential expression of secondary metabolism genes occurs following nutrient depletion (34), but the transcriptional control mechanisms that govern the onset of secondary metabolites are still obscure (29). The *rpoZ* gene of *Streptomyces kasugaensis* has been shown to be required for antibiotic production and morphological differentiation but is not essential for growth (21). A DNA fragment containing the *rpoZ* gene was shown to complement an *S. kasugaensis* pleiotropic mutant deficient in aerial mycelium formation and kasugamycin biosynthesis. Although sigma factors in *Streptomyces* have received considerable attention in relation to the expression of antibiotic biosynthetic genes (9, 19, 20), the role of the RNAP ω subunit is still obscure.

The expression of many genes involved in antibiotic biosynthesis is negatively controlled by the phosphate concentration in the medium (reviewed in references 28 and 30). Limitation of inorganic phosphate produces drastic changes in primary metabolism and triggers the onset of secondary metabolism (34).

Phosphate control over the expression of several genes involved in primary or secondary metabolism (37) is mediated by the two-component system PhoR-PhoP (45, 46). Binding of the response regulator PhoP to specific sequences (named PHO boxes) in the promoter regions of phosphate-controlled genes allowed us to identify the consensus binding sequence of the PhoP operator in *Streptomyces coelicolor* (47).

Bioinformatic studies revealed that the *rpoZ* gene has a highly conserved PHO box in its promoter region. Taking into account the putative role of RpoZ in the transcription of genes involved in differentiation and secondary metabolism biosynthesis and its possible regulation by PhoP, it was of utmost interest to study the role of *rpoZ* in antibiotic biosynthesis and morphological differentiation in *S. coelicolor* and its possible regulation by PhoP. In this work, we report the deletion of *rpoZ* via the REDIRECT technique (16), phenotype restoration when a copy of the *rpoZ* wild-type allele is introduced, and *in vivo* and *in vitro* studies on the effect of PhoP on the expression of the *rpoZ* gene. The results indicate an important role of the RpoZ protein in sporulation and antibiotic biosynthesis. The work also establishes *rpoZ* as a new member of the *pho* regulon in *S. coelicolor*.

* Corresponding author. Mailing address: Institute of Biotechnology (INBIOTEC), Avda. Real 1, 24006 León, Spain. Phone: 34987210308. Fax: 34987210388. E-mail: jf.martin@unileon.es.

† Supplemental material for this article may be found at http://aem.asm.org/.

▽ Published ahead of print on 9 September 2011.

MATERIALS AND METHODS

Bacterial strains, plasmids, and growth conditions. *Streptomyces coelicolor* strains M145 (18) and INB201 (Δ*phoP*) (40) and *gmk*::Tn*5062* and Δ*rpoZ* mutants (this study) were manipulated according to standard procedures (18). TBO medium (17) was used to obtain spores. *S. coelicolor* liquid cultures were grown in defined MG-3.2 medium containing starch (Scharlau) (50 g liter^{-1}), glutamate (8.83 g liter^{-1}), and phosphate (3.2 mM) (39). One hundred milliliters of MG-3.2 medium in 500-ml baffled flasks was inoculated with 10^6 spores ml^{-1} and incubated at 30°C and 300 rpm for dispersed and reproducible growth. Samples for antibiotic production and growth were taken after 35, 47, 52, 57, 70, 80, and 100 h of growth, and samples for promoter activity determination were taken after 41, 44, 47, 49, and 65 h of growth.

For the solid cultures TBO, MS, ISP4, TSA, R5, and YPD media (18) were inoculated with a suspension of 10^8 spores ml^{-1} and grown at 30°C (normal conditions) or 40°C (for temperature resistance assay).

***rpoZ* disruption by gene replacement.** The *rpoZ* deletion mutant was obtained by REDIRECT technology (16). Two primers (rpoZ-F [5′-CCGACCGAATCT TTCCCATCCATCGGAAGGTAGAGCGTGATTCCGGGATCCGTCGACC] and rpoZ-R [5′-GCAAGGCTGAAGATATTACCGCCGATGCTGCTGGTAC TATGTAGGCTGGAGCTGCTTC]) were designed for the amplification of the apramycin resistance cassette of pIJ774. The PCR product was electroporated in *E. coli* BW25113/pIJ790 carrying the cosmid St9C5, an *S. coelicolor* cosmid containing target SCO1478. Since *E. coli* BW25113/pIJ790 has a high recombination activity, replacement of the *rpoZ* coding region by the apramycin resistance cassette takes place with high efficiency. The recombinant cosmid was transformed in *E. coli* ET12567/pUZ8002 and then transferred to *Streptomyces* by conjugation. Deletion mutants were selected by their Apr^r Kn^s phenotype and confirmed by PCR and Southern hybridization.

Complementation of Δ*rpoZ* strains. A 550-bp fragment of *S. coelicolor* M145 that contains the *rpoZ* gene with its promoter and terminator sequences was amplified with primers RPOZ-Cu1 (5′-GGGCCTCTAGATAAGTCAGCGCA) and RPOZ-PD (5′-ACGAGCTGGATCCGCAGGCTCA), which had been modified with XbaI and BamHI restriction sites, respectively. The PCR product was cloned into pRA (36), an integrative conjugative plasmid. In order to introduce the complementation plasmid in the apramycin-resistant Δ*rpoZ* mutant strain, a 1.4-kb fragment containing the Tn*5*/Neo resistance gene was cloned in the EcoRV site of pRA. The complementation was confirmed by Southern hybridization using as probes the complementing DNA fragment (550 bp) and an internal fragment of the Apr^r gene (0.9 kb).

Disruption of the *gmk* gene. SCO1479 (*gmk*)-disrupted mutants were constructed using the apramycin-resistant Tn*5062* insertion 7D08.2.A11 as described by Fernández-Martínez et al. (10). The exconjugants were checked by Southern blot hybridization using the Tn*5062* itself (3,442 bp) as a probe.

Growth, phosphate, and antibiotic determinations. Dry weight determinations were made by drying pellets of 2 ml of cultures after washing twice with MilliQ water. The phosphate concentration of the culture supernatants was measured with the malachite green assay (24). Antibiotic assays were performed as described by Kieser et al. (18). Calcium-dependent antibiotic (CDA) was determined using bioassays with *Bacillus mycoides* CECT 4128.

Cloning of the *rpoZ* promoter region for luciferase assays. The *rpoZ* promoter region was amplified by PCR using total DNA as the template and the primers RPOZ-PD (5′-ACGAGCTGGATCCGCAGGCTCA) and RPOZ-PU (5′-GAG GACATATGCTACCTTCCGAT). The 246-bp amplified fragment encompasses the intergenic region between SCO1479 and SCO1478 (from position −62 to −4 with respect to the translation start triplet of SCO1478) and the last 176 nucleotides (nt) of the SCO1479 coding region. The BamHI and NdeI cloning sites (underlined) were introduced in the primer sequences of RPOZ-PD and RPOZ-PU, respectively, and cloned into the BamHI-NdeI pLUXAR-neo digested vector (40) to obtain (pLUX-*rpoZ*), which was confirmed by sequencing.

The *luxAB* activity driven from the promoter was determined in a Sirius V3.2 luminometer (Berthold Technologies). The samples for the luciferase assay were kept on ice until all were collected, and then 500 μl of each sample was mixed with 250 μl of 0.1% *n*-decanal by injection and measured in a raw data program with an integration time of 20 s after a 5-s delay time step. Measurement units are given as relative light units (RLU) per second.

EMSA. For the electrophoretic mobility shift assay (EMSA) analyses, the 246-bp fragment containing the *rpoZ* promoter was cloned into the vector pGEM-T to obtain pGEM-*rpoZ*. The fluorescent DNA probe was obtained by PCR using pGEM-*rpoZ* as the template and 6-carboxyfluorescein (6-FAM)-labeled primers (6FAM-T7 and 6FAM-SP6). The labeled probe (425 bp) was purified from an agarose gel using GFX columns. The conditions for DNA-protein binding were described previously by Sola-Landa et al. (46). For the control competition reactions, the unlabeled 246-bp fragment containing the *rpoZ* promoter (specific) and an unlabeled 1,190-bp fragment internal to the SCO1661 coding region (nonspecific) were used.

Samples were run in 0.5× Tris-borate-EDTA (TBE) buffer on a 5% polyacrylamide native gel for 2 h at 80 V using a Bio-Rad Mini Protean III instrument. After the run, the gel was scanned in an Ettan DIGE Imager charge-coupled device (CCD) camera (GE Healthcare) and analyzed using the software ImageQuant TL.

Primer extension analysis. RNA samples were taken at 48 h from *S. coelicolor* M145 (wild type) and INB201 (Δ*phoP*) MG-3.2 cultures. The isolation of RNA was performed with the RNeasy Midikit (Qiagen). RNA concentration and quality were checked using a NanoDrop ND-1000 (Thermo Fisher Scientific) and a 2100 Bioanalyzer (Agilent). The transcription start site was determined as described by Santos-Beneit et al. (39) using Superscript III reverse transcriptase (Invitrogen) and the *rpoZ*-FAM + 99 primer (5′-CGCGTAGATCACGAGGC TGTACTTC), which is complementary to the *rpoZ* coding region from nucleotide +75 to +99.

Electron microscopy. Microscopic morphological observations were performed by scanning electron microscopy (JSM-6480 LV; JEOL, Japan), from 6-day-old MS plates (30°C). Glutaraldehyde-fixed samples were dehydrated through a graded ethanol series and critical-point dried in a Bal-Tec (Liechtenstein) CPD 030 critical-point dryer using liquid CO_2. Samples were then coated with a 2-nm gold layer in a Balzers Union (Liechtenstein) SCD 004 sputter coater.

Information theory analysis of binding sites. To evaluate the potential binding of PhoP, we calculated the individual information content (43) of each 11-nt stretch using the weight matrix of model I of Sola-Landa et al. (47). This weight matrix gathers the information of 37 direct-repeat units (DRu) that form the core of experimentally demonstrated PhoP operators.

RESULTS

The SCO1478 open reading frame (ORF) encodes a small protein homologous to RpoZ. The SCO1478 gene of *S. coelicolor* encodes a small protein (90 amino acids) with a predicted mass of 9.7 kDa that is homologous to the RpoZ of *S. kasugaensis* (98% identity) (21) and to a hypothetical protein identified in the genomes of *Streptomyces griseus* and other *Streptomyces* species, but it is not similar to the WhiG-like sigma factor designated RpoZ in *Streptomyces aureofaciens* (22, 23) (see Discussion). The RpoZ protein contains a PRK02950 motif, which is characteristic of the DNA binding domain of the RNA polymerase ω subunit.

In *E. coli* the *rpoZ* gene is linked to the *spoT* gene (12), encoding a pyrophosphatase that controls the ppGpp levels. As shown in Fig. 1, the *S. coelicolor rpoZ* gene is located downstream of a guanylate kinase gene (*gmk*) that is involved in the biosynthesis of guanine nucleotides (35). Since the *gmk-rpoZ* arrangement is kept in *E. coli* and in *S. coelicolor* (Fig. 1), the possible role of *gmk* in differentiation and secondary metabolite production was also investigated by gene disruption (see below).

Deletion of the *rpoZ* gene alters the phenotype of the mutant. In order to elucidate the role of *rpoZ*, the gene was deleted using the REDIRECT technique. For this purpose, cosmid St9C5, containing the pIJ774 cassette replacing *rpoZ*, was transformed into *E. coli* ET12567/pUZ8002 (see Materials and Methods). After conjugation into *S. coelicolor*, four Apr^r Kn^s transformants (named T107, T150, T162, and T165) were selected. The deletion of the *rpoZ* gene in these four transformants was confirmed by PCR and Southern hybridization. The four Δ*rpoZ* transformants behaved similarly, and one of them, T165, was selected for further studies. Complementation of the Δ*rpoZ* mutant (T165) was performed by conjugation with *E. coli* ET12567/pUZ8002 carrying the construction pRA-*rpoZ*

FIG. 1. Physical map of the *S. coelicolor* DNA region containing the *rpoZ* gene (SCO1478). Note the linkage to the *gmk* gene (SCO1479), encoding a putative guanylate kinase. For comparison, the *E. coli* DNA region containing the *rpoZ*, *gmk*, and *spoT* genes is shown at the bottom.

(see Materials and Methods), in which the *rpoZ* gene is expressed from its own promoter and carries its own terminator sequence. The complementation was also confirmed by PCR and Southern hybridization.

To determine the phenotype of the Δ*rpoZ* mutant, the parental M145, Δ*rpoZ* (T165), and complemented (C1) strains were grown on several media. After 2 days of growth, the onset of actinorhodin (ACT) production was clearly precocious in the Δ*rpoZ* strain on MS medium (Fig. 2A). On the other hand, *S. coelicolor* Δ*rpoZ* showed delayed growth on all media tested, especially TBO and ISP4 (Fig. 2B), at this time. After 4 days of growth, actinorhodin production was already observed in both the wild-type and complemented strains on R5, TSA, and ISP4 but not on YPD, MS, and TBO. On the other hand, the Δ*rpoZ* strain produced significant amounts of actinorhodin on R5, ISP4, MS, and TBO, although not on TSA (Fig. 2C). Sporulation of the Δ*rpoZ* mutant was delayed in comparison to those of the parental and complemented strains (Fig. 2B and C). After 6 days, all strains were able to sporulate on TBO, MS, and ISP4, although the spores of the Δ*rpoZ* mutant remained white (Fig. 2D). This white phenotype of the mutant remained after 2 weeks of growth. Another interesting observation was the sensitivity of *S. coelicolor* Δ*rpoZ* to high temperatures; indeed, when the temperature was increased to 40°C, the mutant was impaired in aerial mycelium formation, showing a bald phenotype, while the wild type was still able to sporulate (Fig. 2E). However, despite the lack of spore pigmentation and the lower resistance to heat stress, the mutant spores were viable and showed normal morphology, as confirmed by electron microscopy (Fig. 3).

To test if the putative guanylate kinase gene (*gmk*) had any role in differentiation or antibiotic production, this gene was disrupted as described in Materials and Methods. Disruption of *gmk* did not alter the phenotype of the mutant (data not shown), excluding a role of this gene in the control of growth, differentiation, or secondary metabolism.

In summary, on most of the solid media tested, deletion of *rpoZ* produced a retardation of growth, a lack of the gray pigmentation, and an early onset of actinorhodin biosynthesis.

ACT and RED pigment production is drastically altered in Δ*rpoZ* liquid cultures. In order to quantify the effect of the *rpoZ* deletion on growth and antibiotic production in submerged cultures, the Δ*rpoZ* mutant, M145, and the complemented *rpoZ* (C1 and C2) strains were grown in liquid MG-3.2 medium (38, 39, 40, 41, 42). Phosphate is depleted in this medium (the residual level is below 0.1 mM) after 44 h of growth, time in which the *pho* regulon genes are induced and the onset of secondary metabolism takes place (39, 40).

As shown in Fig. 4, growth of the Δ*rpoZ* mutant was slower than that of the parental and complemented strains during the first 70 h of culture. In fact, the phosphate in the medium was depleted in the mutant cultures 10 h later than in the control cultures (indicated by vertical lines in Fig. 4A). However, the final biomass was higher in the mutant strain than in the parental and complemented strains (Fig. 4A). When the cultures were observed under the optical microscope, differences were observed between the wild-type and mutant strains in terms of the shape and complexity of the mycelial pellets. While the parental strain developed branches of mycelium around the initial pellets, which grow throughout the time culture, no branch formation was observed in the Δ*rpoZ* mutant cultures (see Fig. S1 in the supplemental material). This observation points toward a role of RpoZ in the control of mycelium development in *S. coelicolor* in both liquid and solid cultures (26).

In relation to the antibiotic synthesis in liquid cultures, there was a burst of actinorhodin (ACT) production in the Δ*rpoZ* mutant at the first stages of culture growth, in contrast to the case for the parental strain, in which antibiotic production took place after 47 h (Fig. 4B). The volumetric ACT values for the parental strain increased from 1.7 ± 0.6 μg ml^{-1} at 47 h to 254 ± 27 μg ml^{-1} at 70 h, in contrast to the case for the Δ*rpoZ* mutant, where the volumetric ACT values did not change from 47 h (28.7 ± 0.3 μg ml^{-1}) to 70 h (29.4 ± 1 μg ml^{-1}). This indicates that the synthesis of ACT is precocious in the mutant strain but that it fails to maintain the normal production rate after 47 h. This phenomenon agrees with the clear burst of ACT production observed in complex MS and TBO solid media, where the Δ*rpoZ* mutant strain started to produce ACT sooner than the parental strain, in spite of the significant delay in growth of the mutant (Fig. 2A and C). In conclusion, the onset of actinorhodin biosynthesis took place earlier in the Δ*rpoZ* mutant, although maximum ACT values were quite low in comparison to those in the parental M145 strain.

A more drastic effect of the *rpoZ* deletion on undecylprodigiosin (RED) production was observed. Almost no detectable synthesis of the RED pigment was observed in the Δ*rpoZ* strain, at least until very late time points, when a low production of this pigment took place (Fig. 4C). Strikingly, while in the parental strain ACT production and RED production took

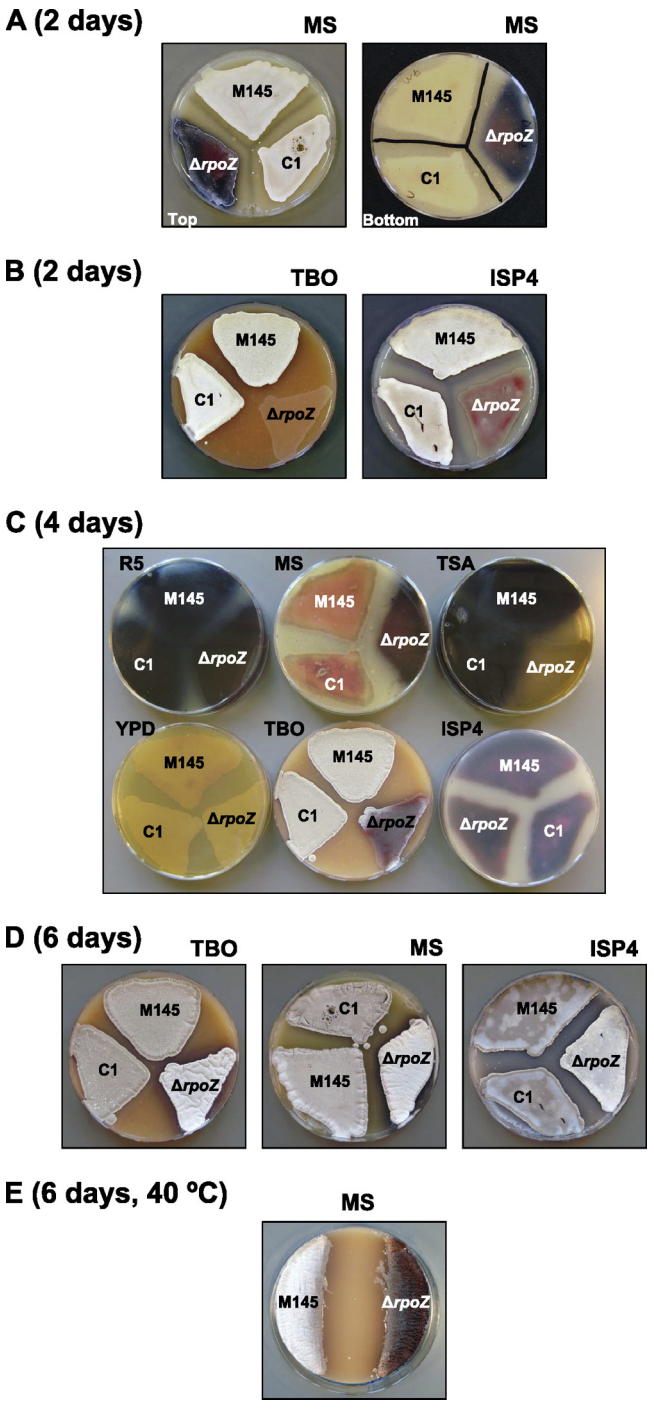

FIG. 2. Phenotypic effect of the Δ*rpoZ* mutation on growth, sporulation, and pigmentation on six different solid media: MS, TBO, ISP4, R5, TSA, and YPD. (A) MS plate after 2 days of growth. Left image, top view. Right image, bottom view. Note the precocious pigmentation of the Δ*rpoZ* strain in this medium. (B) Top view of TBO and ISP4 plates after 2 days of growth. Note the delay in growth of the Δ*rpoZ* mutant on both media. (C) Bottom view (except top view for TBO) of R5, MS, TSA, YPD, TBO, and ISP4 plates after 4 days of growth. Note the changes in pigmentation of the Δ*rpoZ* mutant on MS, TSA, and TBO plates and the delay in sporulation of the mutant on TBO medium. (D) Top view of TBO, MS, and ISP4 plates after 6 days of growth. Note the lack of spore gray pigmentation of the Δ*rpoZ* mutant in all plates. (E) Top view of an MS plate after 6 days of growth at 40°C. Note the lack of sporulation of the Δ*rpoZ* mutant.

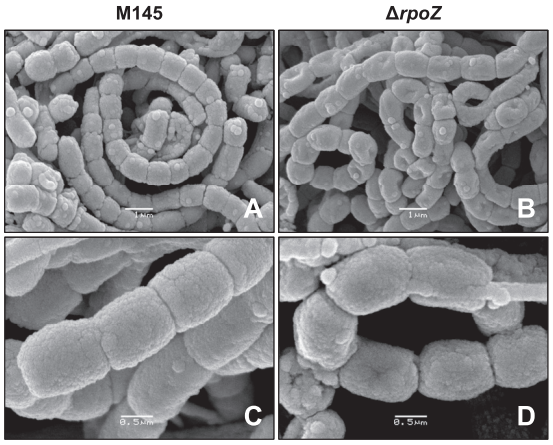

FIG. 3. Scanning electron microscopy of spores of the parental (M145) and Δ*rpoZ* mutant strains after growth on MS for 6 days at 30°C. Magnifications, ×13,000 (A and B) and ×30,000 (C and D).

place almost simultaneously, with RED production closely followed by ACT production, in the mutant the synthesis of these antibiotics occurred in very separate stages of the culture (with the ACT pigment produced first and the RED one later).

Almost full restoration of ACT production and partial restoration of RED production were observed in the complemented strain (Fig. 4B and C). This lack of full restoration is due to the effect of integration of the plasmid on ACT and RED production, as was shown when the plasmid without the complementation cassette was introduced in the wild-type strain (Fig. 4B and C). This indicates that the drastic reduction in formation of these secondary metabolites is due to the absence of a functional RpoZ (see Discussion). Not all secondary metabolites are regulated in the same manner. The production of calcium-dependent antibiotic (CDA) in nutrient agar was slightly increased in the Δ*rpoZ* mutant strain compared to the parental strain, and its production was restored to the parental levels in the complemented strain (Fig. 5).

The *gmk*-disrupted mutant was also tested for ACT, RED, and CDA production and did not show any significant difference with respect to the parental strain, excluding a polar effect of *rpoZ* deletion on the *gmk* mutant phenotype (data not shown).

Binding of PhoP to the promoter region of *rpoZ*. Inorganic phosphate is known to control expression of genes involved in both primary and secondary metabolism. Many of the primary metabolism genes are controlled by direct binding of PhoP to their promoter regions (37, 47), whereas secondary metabolism genes are regulated through signal transduction cascades involving pathway-specific regulators (29, 40).

Bioinformatic studies indicated that the region upstream of *rpoZ* contains two direct repeat units, designated DRu-1 and DRu-2, i.e., a PHO box. They are adjacent and located at 33 nt from the *rpoZ* translation start triplet. The individual information content (the *R*i value) (43) of each 11-nt DRu obtained using model I of the PhoP binding site (47) indicates that the two DRus have a high score (9.7 and 7.3 bits for DRu-1 and DRu-2, respectively), although these values were lower than in the consensus PHO box (*R*i 14.6 bits) since the second nucleotides of both DRu-1 and DRu-2 did not match the consensus

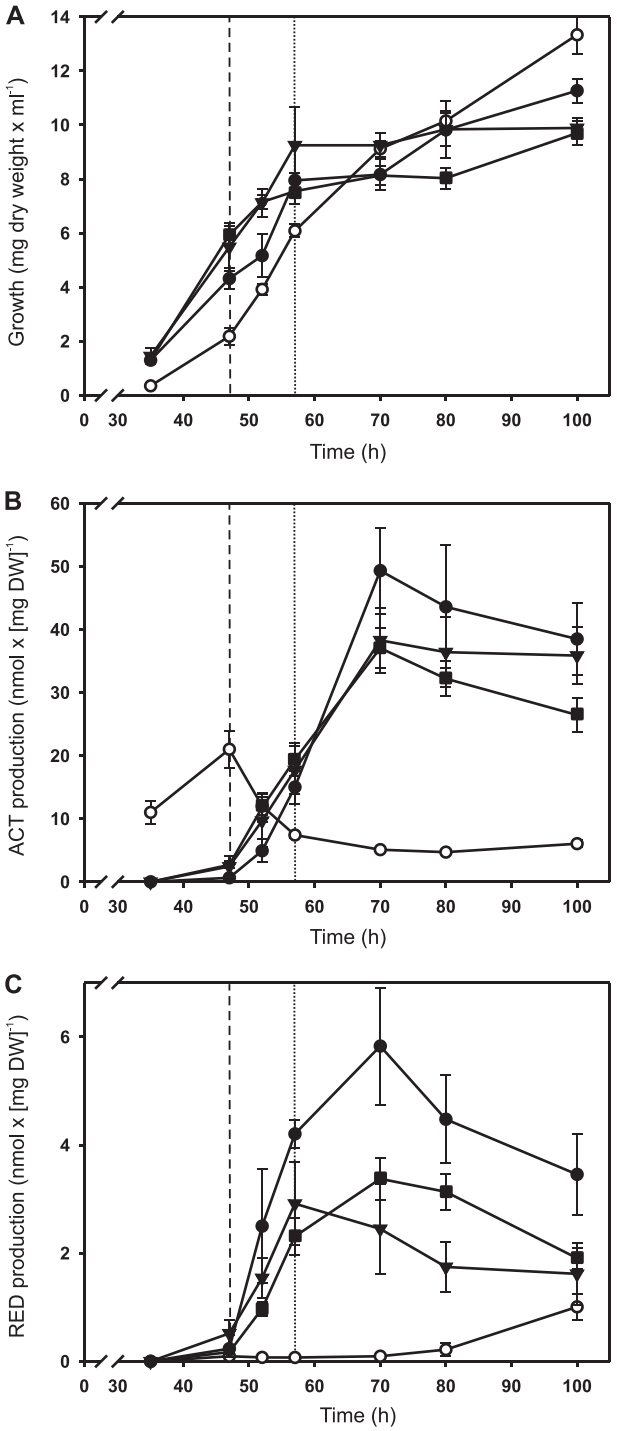

FIG. 4. Growth and production of actinorhodin (ACT) and undecylprodigiosin (RED) by the parental strain M145, the Δ*rpoZ* mutant, the complemented mutant strains (C1 and C2), and strain M145 plus the plasmid without the complementation cassette (control) in MG-3.2 medium. (A) Dry weight; (B) ACT production; (C) RED production. Black circles, strain M145; black squares, M145 control; white circles, Δ*rpoZ* mutant; black triangles, complemented strains. The vertical lines indicate when phosphate is depleted in the medium (<50 μM) in both parental (dashed lines) and Δ*rpoZ* (dotted lines) cultures. Error bars correspond to the standard errors of the means for three biological replicates in M145 and Δ*rpoZ* cultures and four replicates for the complemented strains (two cultures of each complemented strain).

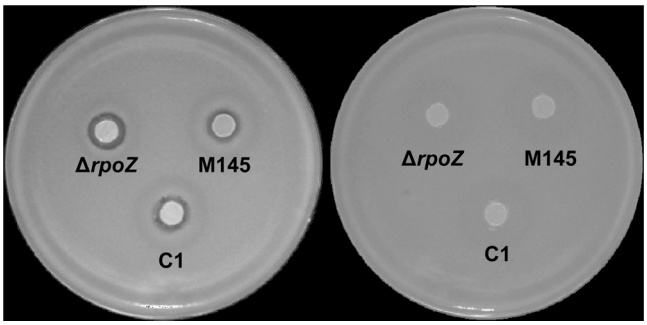

FIG. 5. Effect of *rpoZ* deletion on CDA production. For the bioassay, strain M145, the Δ*rpoZ* mutant, and C1 (Δ*rpoZ* mutant complemented with the wild-type *rpoZ*) were grown on nutrient agar for 48 h. Agar plugs (5 mm in diameter) were then transferred to soft nutrient agar inoculated with *Bacillus mycoides*. The plate on the left was supplemented with 17 mM calcium nitrate to induce CDA activity. The plate on the right, without calcium nitrate, acts as a control.

T nucleotide. This feature is also observed in the promoter region of one of the major sigma factor-encoding genes (*hrdA*) in *S. coelicolor*, which has been previously shown to be bound and repressed by PhoP (37, 47) (Fig. 6A). Therefore, binding of PhoP to the 223-nt DNA fragment carrying the *rpoZ* promoter region was tested. As shown in Fig. 6B, binding of PhoP

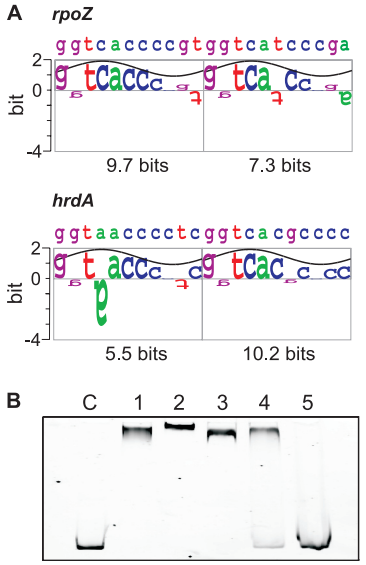

FIG. 6. (A) Individual information analysis of the PhoP binding sites in the *rpoZ* and *hrdA* promoter regions using the sequence walker method (43) and the model I weight matrix of Sola-Landa et al. (47). Boxes contain the individual information content (*R*i, bits) of each 11-nt direct repeat unit (DRu). The height of the letters represents the *R*i contribution of each position to the total information content. Letters extending downward represent unfavorable protein-DNA contacts. Note that in both cases the second base is unfavorable for each of the DRus. (B) Electrophoretic mobility shift assays of the *rpoZ* promoter with the glutathione *S*-transferase (GST)-PhoP^{DBD} protein and competition with unlabeled probe. Lane C, control (labeled probe without protein). Lanes 1 to 5, labeled probe with protein at 2 μM (lane 1) and 4 μM (lane 2), 4 μM protein and a 500× excess of unlabeled unspecific probe (lane 3), 4 μM protein and a 100× excess of unlabeled specific probe (lane 4), and 4 μM protein and a 500× excess of unlabeled specific probe (lane 5).

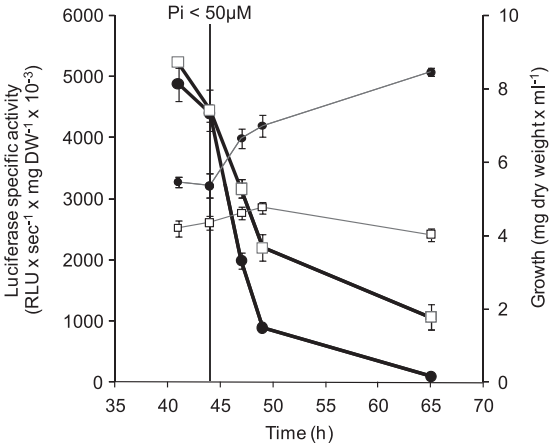

FIG. 7. Expression of the *rpoZ* promoter coupled to the *luxAB* reporter genes in *S. coelicolor* M145 (black circles) and INB201 (Δ*phoP*; white squares) strains in MG-3.2 medium. Luciferase specific activity (black lines, left *y* axis) and growth (gray lines, right *y* axis) are shown. The time when the phosphate in the medium is depleted (<50 μM) in both M145 and INB201 cultures is represented with a black vertical line. Error bars correspond to the standard errors of the means for four biological replicates (two replicates of two different exconjugants per condition).

to this region was clearly observed, giving rise to one shifted band (DNA-PhoP complex), as expected for a core-core (CC)-type operator (47). This result suggests that expression of *rpoZ* is modulated by PhoP.

PhoP control of *rpoZ* expression. To check the *in vivo* effect of the PhoP binding on *rpoZ* expression, the promoter of this gene was coupled to the *luxAB* genes and introduced into both the parental and Δ*phoP* strains as described in Materials and Methods. The cultures for the luciferase analysis contained a limiting phosphate concentration (MG-3.2) in order to achieve the PhoP response once this nutrient is depleted from the medium. The results showed that when the phosphate became depleted (vertical line in Fig. 7), the *rpoZ* promoter activity, which was identical in both strains until that time, was higher in the *S. coelicolor* Δ*phoP* mutant for as long as the cultures went on. A similar difference occurred in terms of growth; the Δ*phoP* strain was not able to continue growing after 44 h, while the parental strain continued growing at least till 65 h.

This higher expression of *rpoZ* in the Δ*phoP* strain points to a negative role of PhoP in the regulation of the *rpoZ* gene. This observation is also supported by transcriptomic studies using the M145 and Δ*phoP* mutant strains, in which the *rpoZ* expression in the Δ*phoP* mutant increased an average of 3.7-fold with respect to that in the wild type (see Fig. S2 in the supplemental material).

Characterization of the *rpoZ* promoter. In order to elucidate the molecular basis of the negative role of PhoP in *rpoZ* expression, the transcription start point (TSP) of *rpoZ* was determined by primer extension analysis. The aim of the experiment was to determine the position of the PHO box with regard to the TSP and to check whether the TSP is the same in the wild-type and Δ*phoP* strains. For this purpose, RNA samples from 48-h MG-3.2 phosphate-limited cultures were used. As shown in Fig. 8, the same TSP was obtained in both the wild-type and Δ*phoP* strains, and the PHO box was located at positions −54 to −33.

As shown in Fig. 8, the TSP of *rpoZ* coincides with the first nucleotide (G) of its translation start triplet. Although the majority of archaeal transcripts are leaderless, this is not the case with bacterial transcripts (3). In any case, at least 11 leaderless transcripts of different *Streptomyces* species are described in the review by Strohl (48). Of these 11 transcripts, only one has a GUG as the translation start triplet, so this feature does not seem to be usual in *Streptomyces*. In all com-

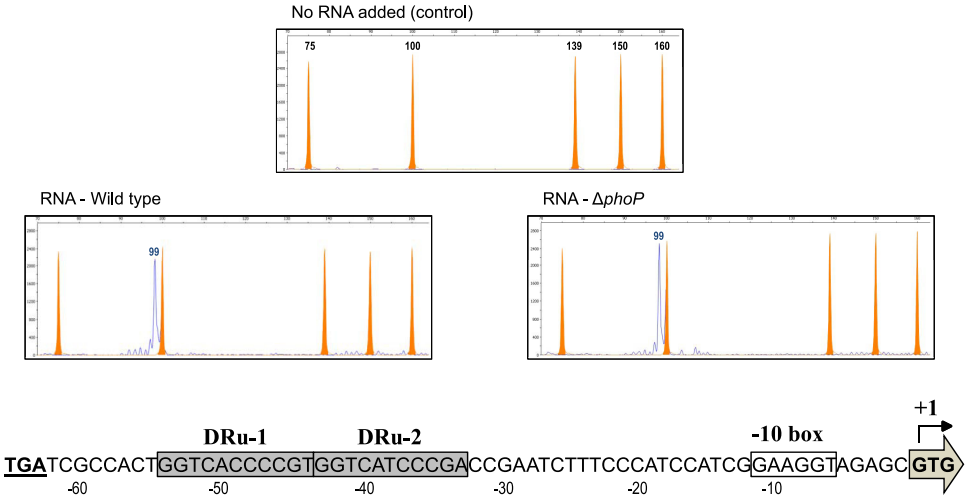

FIG. 8. Primer extension analysis of the *rpoZ* promoter using automated fluorescent capillary electrophoresis. Primer extension reactions were done with the *rpoZ*-FAM + 99 primer using both wild-type and Δ*phoP* RNA samples. Results of a control reaction in which no RNA was added are shown in the upper fluorogram. The filled traces represent the LIZ-500 standard that was included in each sample to determine the size of the extension product (unfilled trace). Note that in both the wild-type and Δ*phoP* RNA samples, the same extension product was obtained. The box at the bottom summarizes the promoter elements of the gene. The translation start triplet of *rpoZ* and the translation end triplet of the upstream gene are in boldface. The transcription start point (+1) is indicated with an arrow above. The putative −10 element and the DRus that form the PhoP operator are boxed. The position with respect to the translation start triplet is indicated under the nucleotide sequence.

piled promoters, the −10 box ends with a T (48). Taking into account this feature and also the presence of an A (86%) in the second position of the hexamer and the presence of a purine nucleotide in the fourth and fifth positions (69% and 72%, respectively), we have identified the hypothetical −10 element of the *rpoZ* promoter (Fig. 8). However, no obvious −35 hexamer was found around the −35 region of the *rpoZ* promoter, and the PHO box was located upstream of this region. In other *pho* genes, the PHO box is located in the −35 region. PhoP usually acts as a transcriptional activator when it binds to the −35 region. In our case, PhoP acts a transcriptional repressor. This might occur by a change in the conformation of the DNA that affects the transcription process (see Discussion).

DISCUSSION

All bacterial RNA polymerases consist of five subunits, α_2 (two identical monomers), β, β′, and ω, which perform DNA-dependent transcription (14). In addition, a variety of sigma (σ) factors are used in the recognition of different promoters (9, 19, 20, 27). The role of the omega subunit of the bacterial RNAP complex has remained obscure for decades. *In vitro* studies with *E. coli* revealed that the ω subunit is an important component of RNAP complex, being required to restore functionality to denatured RNAP (33). In fact, the ω subunit has been shown to interact with the $\alpha_2\beta\beta'$ core through binding to the β′ subunit (15). This interaction was also defined when the crystal structure of the *Thermus aquaticus* RNAP was determined (32). The presence of the ω subunit is not strictly required for growth, although *E. coli* mutants lacking the ω subunit show a low growth rate and a lower final cell density (50). On the other hand, a truncated version of RpoZ containing the N-terminal region (51 out of 91 amino acids) is sufficient to interact with the $\alpha_2\beta\beta'$ core, leading to a full growth rate of the complemented strain (15).

The deletion of the *rpoZ* gene in *Mycobacterium smegmatis* (31) produced a fragmentation of the β′ subunit, although the fragments remained associated with the RNAP core. This mutant showed a reduced growth rate and abnormal colony morphology and pigmentation (31).

The *S. coelicolor* 90-amino-acid RpoZ protein is highly conserved in all sequenced *Streptomyces* genomes. No other *rpoZ*-like gene was found in the genome of *S. coelicolor*. Surprisingly, an unrelated gene encoding a 278-amino-acid sigma factor homologous to WhiG, which also influences sporulation, was named *rpoZ* in *Streptomyces aureofaciens* (22, 23). However, the homology of *S. coelicolor* RpoZ to the ω subunits of *E. coli* (12), *M. smegmatis* (31), *S. kasugaensis* (21), and other bacteria clearly indicates that the 90-amino-acid protein encoded by SCO1478 is the authentic ω subunit of this actinomycete.

As shown in this article, deletion of the *rpoZ* gene in *S. coelicolor* causes a reduction of the growth rate, as occurs in *E. coli* and *M. smegmatis*. Disruption of the guanylate kinase gene (*gmk*), located upstream of *rpoZ*, had no effect on growth or differentiation. Therefore, *gmk* and *rpoZ* appear to be transcribed independently from each other. The slow-growth phenotype of *S. coelicolor* Δ*rpoZ* in several solid and liquid media suggests that the RNAP complex lacking the ω subunit is inefficient in terms of expression of the genes required for a full growth rate. However, it is clear that RpoZ is not essential for growth, since the *rpoZ*-defective mutants are able to reach the same levels of growth in prolonged cultures as the parental strain.

The sporulation process was also affected in the Δ*rpoZ* mutant, although viable spores, with normal morphology, are formed. However, the spores of the mutant lack the typical gray pigment associated with *S. coelicolor* and other *Streptomyces* spores. In addition to the white phenotype, the Δ*rpoZ* mutant is less resistant to temperature stress than the parental strain. A bald phenotype (no aerial mycelium formation) is obtained when the mutant strain is grown at 40°C. A role of RpoZ in resistance to heat stress in *E. coli* was also reported. In this bacterium, overproduction of RpoZ suppressed the temperature-sensitive phenotype of *rpoZ* mutants (32).

In this work we show that the deletion of *rpoZ* in *S. coelicolor* has a very strong effect on antibiotic biosynthesis, particularly on undecylprodigiosin, almost preventing its expression. Kojima and coworkers (21) observed a similar effect on the biosynthesis of the aminoglycoside kasugamycin and proposed that this might be a general effect, also affecting secondary metabolites other than aminoglycosides. Indeed, in *S. coelicolor*, the deletion of *rpoZ* affected not only the biosynthesis of the proline-derived undecylprodigiosin but also that of the polyketide actinorhodin, the lipopeptide CDA, and the gray pigment associated with spores, suggesting that RpoZ modulates the expression of different secondary metabolites. These unrelated metabolites were affected differently by the deletion of *rpoZ*; undecylprodigiosin and the gray pigment were almost abolished in the Δ*rpoZ* mutant, whereas CDA synthesis increased. On the other hand, production of actinorhodin was impaired after an initial burst in the first stages of the culture. The precocious production of actinorhodin by the Δ*rpoZ* mutant may be explained as the result of defective RNAP complex formation which induces a low growth rate that triggers a burst of this antibiotic. These differences are likely to be due to the distinct organization and nucleotide sequences of promoters in the actinorhodin, undecylprodigiosin, or CDA clusters that affect their interaction with the RNAP complex and the ω subunit.

The molecular mechanism of interaction of the RNAP complex with promoters of genes controlling secondary metabolism is also modulated by the action of specific DNA binding proteins such as PhoP or AfsR (40). AfsR seems to act by recruiting the RNAP complex to interact with higher affinity with those AfsR-regulated promoters (49). AfsR is, indeed, a positive regulator of *afsS* (encoding a sigma factor-like small protein) that triggers expression of the pathway-specific regulators ActII-ORF4 and RedD (11).

PhoP recognizes a DNA binding sequence similar to that of AfsR (40) and appears to act by a similar mechanism, recruiting the RNAP complex for interaction with the *afsS* promoter. In *E. coli* and *Bacillus subtilis*, the PhoB protein (homologous to the *Streptomyces* PhoP) also interacts with the RNAP holoenzyme (5, 25). In summary, the RpoZ protein may affect expression of secondary metabolite genes by interaction with the core RNAP and with wide-domain regulators such as AfsR or PhoP.

As shown in this work, PhoP binds to the *rpoZ* promoter, in agreement with the presence in its promoter of a consensus

PHO box. Two direct repeats, DRu-1 and DRu-2, are adjacent, forming a class I (CC) operator (47). Although both DRus have an unconserved nucleotide in the second position, PhoP was shown to bind the promoter with high affinity. The binding of PhoP to this region formed a single DNA-protein complex, in agreement with the behavior of class I operators. The effect of PhoP on this promoter is negative, since the promoter activity was higher in the Δ*phoP* mutant than in the parental strain.

According to Browning and Busby (4), there are three general mechanisms of transcriptional repression. In the first mechanism, the repressor binds in or close to the core of the promoter elements and produces a steric hindrance of RNA polymerase binding. In the second, the repressor binds to promoter-distal sites and does not prevent binding of RNA polymerase to the promoter but instead interferes with postrecruitment steps in transcription initiation. In the third mechanism, the repressor functions as an antiactivator.

We have previously described that PhoP acts as a repressor with the first mechanism mentioned above. Thus, PhoP represses *pitH2* transcription when it binds overlapping the −10 element (39). PhoP also has been shown to function as an antiactivator (third mechanism). PhoP represses the *glnA* and *afsS* genes competing with the binding sites of the transcriptional activators GlnR and AfsR (38, 40, 42). In this study, we also describe PhoP acting as a transcriptional repressor according to the second mechanism. Thus, *rpoZ* expression is slightly decreased when PhoP binds upstream of the promoter elements. Only the steric hindrance mechanism (where the binding of the RNA polymerase is prevented when PhoP binds to the −10 hexamer) seems to produce a drastic repression effect on the transcription of the genes controlled by this protein.

ACKNOWLEDGMENTS

This work was supported by grants from the CICYT Consolider Project Bio2006-14853-O2-1 (Ministry of Science and Innovation, Madrid) and the ERA Sysmo STREAM Project (GEN2006-27745-E/SYS). Miriam Martínez-Castro received a fellowship from the FPU program (Ministry of Education, Spain).

We thank P. Dyson and M. Evans for insertion 7D08.2.A11, E. Wellington and the STREAM consortium for transcriptional data for the *rpoZ* gene in the Δ*phoP* mutant, and B. Martín, J. Merino, and A. Mulero for excellent technical assistance.

REFERENCES

1. **Bentley, S. D., et al.** 2002. Complete genome sequence of the model actinomycete *Streptomyces coelicolor* A3(2). Nature **417:**141–147.
2. **Bérdy, J.** 2005. Bioactive microbial metabolites. J. Antibiot. (Tokyo) **58:**1–26.
3. **Brenneis, M., O. C. Hering, Lange, and, J. Soppa.** 2007. Experimental characterization of cis-acting elements important for translation and transcription in halophilic archaea. PLoS Genet. **3:**e229.
4. **Browning, D. F., and S. J. Busby.** 2004. The regulation of bacterial transcription initiation. Nat. Rev. Microbiol. **2:**57–65.
5. **Chen, Y., W. R. Abdel-Fattah, and F. M. Hulett.** 2004. Residues required for *Bacillus subtilis* PhoP DNA binding or RNA polymerase interaction: alanine scanning of PhoP effector domain transactivation loop and alpha helix 3. J. Bacteriol. **186:**1493–1502.
6. **Darst, S. A., E. W. Kubalek, and R. D. Kornberg.** 1989. Three-dimensional structure of *Escherichia coli* RNA polymerase holoenzyme determined by electron crystallography. Nature **340:**730–732.
7. **Darst, S. A., A. M. Edwards, E. W. Kubalek, and R. D. Kornberg.** 1991. Three-dimensional structure of yeast RNA polymerase II at 16 A resolution. Cell **66:**121–128.
8. **Demain, A. L.** 2009. Antibiotics: natural products essential to human health. Med. Res. Rev. **29:**821–842.
9. **Fernández-Martínez, L. T., et al.** 2009. Osmoregulation in *Streptomyces coelicolor*: modulation of SigB activity by OsaC. Mol. Microbiol. **71:**1250–1262.
10. **Fernández-Martínez, L. T., et al.** 2011. A transposon insertion single-gene knockout library and new ordered cosmid library for the model organism *Streptomyces coelicolor* A3(2). Antonie Van Leeuwenhoek **99:**515–522.
11. **Floriano, B., and M. Bibb.** 1996. *afsR* is a pleiotropic but conditionally required regulatory gene for antibiotic production in *Streptomyces coelicolor* A3(2). Mol. Microbiol. **21:**385–396.
12. **Gentry, D., and R. Burgess.** 1989. rpoZ, encoding the omega subunit of Escherichia coli RNA polymerase, is in the same operon as spoT. J. Bacteriol. **171:**1271–1277.
13. **Gentry, D., H. Xiao, R. Burgess, and M. Cashel.** 1991. The omega subunit of *Escherichia coli* K-12 RNA polymerase is not required for stringent RNA control in vivo. J. Bacteriol. **173:**3901–3903.
14. **Gentry, D., and R. R. Burgess.** 1993. Cross-linking of *Escherichia coli* RNA polymerase subunits: identificacion of β′ as the binding site of ω. Biochemistry **32:**11224–11227.
15. **Ghosh, P., A. Ishihama, and D. Chatterji.** 2003. *Escherichia coli* RNA polymerase subunit ω and its N-terminal domain bind full-length β′ to facilitate incorporation into the $\alpha_2\beta$ subassembly. Biophys. Chem. **103:**223–237.
16. **Gust, B., G. L. Challis, K. Fowler, T. Kieser, and K. F. Chater.** 2003. PCR-targeted *Streptomyces* gene replacement identifies a protein domain needed for biosynthesis of the sesquiterpene soil odor geosmin. Proc. Natl. Acad. Sci. U. S. A. **100:**1541–1546.
17. **Higgens, C. E., R. L. Hamill, T. H. Sands, M. M. Hoehn, and N. E. Davis.** 1974. The occurrence of deacetoxycephalosporin C in fungi and streptomycetes. J. Antibiot. **27:**298–300.
18. **Kieser, T., M. J. Bibb, M. J. Buttner, K. F. Chater, and D. A. Hopwood.** 2000. Practical *Streptomyces* genetics. The John Innes Foundation, Norwich, United Kingdom.
19. **Kim, E. S., J. Y. Song, D. W. Kim, K. F. Chater, and K. J. Lee.** 2008. A possible extended family of regulators of sigma factor activity in *Streptomyces coelicolor*. J. Bacteriol. **190:**7559–7566.
20. **Kim, E. S., M. Y. Hahn, Y. Cho, S.-N. Cho, and J. H. Roe.** 2009. Positive and negative feedback regulatory loops of thiol-oxidative stress response mediated by an unstable isoform of σ^R in actinomycetes. Mol. Microbiol. **73:**815–825.
21. **Kojima, I., et al.** 2002. The *rpoZ* gene encoding the RNA polymerase omega subunit, is required for antibiotic production and morphological differentiation in *Streptomyces kasugaensis*. J. Bacteriol. **184:**6417–6423.
22. **Kormanec, J., L. Potúcková, and B. Rezuchová.** 1994. The *Streptomyces aureofaciens* homologue of the *whiG* gene encoding a putative sigma factor essential for sporulation. Gene **143:**101–103.
23. **Kormanec, J., D. Homerová, L. Potúcková, R. Nováková, and B. Rezuchová.** 1996. Differential expression of two sporulation specific sigma factors of *Streptomyces aureofaciens* correlates with the developmental stage. Gene **181:**19–27.
24. **Lanzetta, P. A., L. J. Alvarez, P. S. Reinach, and O. A. Candia.** 1979. Improved assay for nanomole amounts of inorganic-phosphate. Anal. Biochem. **100:**95–97.
25. **Makino, K., et al.** 1996. DNA binding of PhoB and its interaction with RNA polymerase. J. Mol. Biol. **259:**15–26.
26. **Manteca, A., R. Alvarez, N. Salazar, P. Yagüe, and J. Sánchez.** 2008. Mycelium differentiation and antibiotic production in submerged cultures of *Streptomyces coelicolor*. Appl. Environ. Microbiol. **74:**3877–3886.
27. **Mao, X.-M., Z. Zhou, X.-P. Hou, W.-J. Guan, and Y.-Q. Li.** 2009. Reciprocal regulation between SigK and differentiation programs in *Streptomyces coelicolor*. J. Bacteriol. **191:**6473–6481.
28. **Martín, J. F.** 2004. Phosphate control of the biosynthesis of antibiotics and other secondary metabolites is mediated by the PhoR-PhoP system: an unfinished story. J. Bacteriol. **186:**5197–5201.
29. **Martín, J. F., and P. Liras.** 2010. Engineering of regulatory cascades and networks controlling antibiotic biosynthesis in *Streptomyces*. Curr. Opin. Microbiol. **13:**263–273.
30. **Martín, J. F., A. Sola-Landa, F. Santos-Beneit, and A. Rodríguez-García.** 2011. Network mechanisms of phosphate control of primary and secondary metabolism, p. 137–149. *In* P. Dyson (ed.), *Streptomyces*: molecular biology and biotechnology. Horizon Press, Norwich, United Kingdom.
31. **Mathew, R., M. Ramakanth, and D. Chatterji.** 2005. Deletion of the gene *rpoZ* encoding the ω subunit of RNA polymerase, in *Mycobacterium smegmatis* results in fragmentation of the β′ subunit in the enzyme assembly. J. Bacteriol. **187:**6565–6570.
32. **Minakhin, L., et al.** 2001. Bacterial RNA polymerase subunit ω and eukaryotic RNA polymerase subunit RPB6 are sequence, structural, and functional homologs and promote RNA polymerase assembly. Proc. Natl. Acad. Sci. U. S. A. **98:**892–897.
33. **Mukherjee, K., and D. Chatterji.** 1997. Studies on the ω subunit of *Escherichia coli* RNA polymerase—its role in the recovery of denatured enzyme activity. Eur. J. Biochem. **247:**884–889.
34. **Nieselt, K., et al.** 2010. The dynamic architecture of the metabolic switch in *Streptomyces coelicolor*. BMC Genomics **11:**10–19.
35. **Oeschger, M. P., and M. J. Bessman.** 1966. Purification and properties of guanylate kinase from *Escherichia coli*. J. Biol. Chem. **241:**5452–5460.
36. **Pérez-Redondo, R., I. Santamarta, R. Bovenberg, J. F. Martín, and P. Liras.**

2010. The enigmatic lack of glucose utilization in *Streptomyces clavuligerus* is due to inefficient expression of the glucose permease gene. Microbiology **156:**1527–1537.

37. **Rodríguez-García, A., C. Barreiro, F. Santos-Beneit, A. Sola-Landa, and J. F. Martín.** 2007. Genome-wide transcriptomic and proteomic analysis of the primary response to phosphate limitation in *Streptomyces coelicolor* M145 and in a Δ*phoP* mutant. Proteomics **7:**2410–2429.
38. **Rodríguez-García, A., A. Sola-Landa, K. Apel, F. Santos-Beneit, and J. F. Martín.** 2009. Phosphate control over nitrogen metabolism in Streptomyces coelicolor: direct and indirect negative control of glnR, glnA, glnII and amtB expression by the response regulator PhoP. Nucleic Acids Res. 037:3230–3240.
39. **Santos-Beneit, F., A. Rodríguez-García, E. Franco-Domínguez, and J. F. Martín.** 2008. Phosphate-dependent regulation of the low- and high-affinity transport systems in the model actinomycete *Streptomyces coelicolor*. Microbiology **154:**2356–2370.
40. **Santos-Beneit, F., A. Rodríguez-García, A. Sola-Landa, and J. F. Martín.** 2009a. Cross-talk between two global regulators in *Streptomyces*: PhoP and AfsR interact in the control of *afsS*, *pstS* and *phoRP* transcription. Mol. Microbiol. **72:**53–68.
41. **Santos-Beneit, F., A. Rodríguez-García, A. K. Apel, and J. F. Martín.** 2009b. Phosphate and carbon source regulation of two PhoP-dependent glycerophosphodiester phosphodiesterase genes of *Streptomyces coelicolor*. Microbiology **155:**1800–1811.
42. **Santos-Beneit, F., A. Rodríguez-García, and J. F. Martín.** 2011. Complex transcriptional control of the antibiotic regulator *afsS* in *Streptomyces*: PhoP and AfsR are overlapping, competitive activators. J. Bacteriol. **193:**2242–2251.
43. **Schneider, T. D.** 1997. Information content of individual genetic sequences. J. Theor. Biol. **189:**427–441.
44. **Schultz, P., H. Celia, M. Riva, A. Sentenac, and P. Oudet.** 1993. Three-dimensional model of yeast RNA polymerase I determined by electron microscopy of two-dimensional crystals. EMBO J. **12:**2601–2607.
45. **Sola-Landa, A., R. S. Moura, and J. F. Martín.** 2003. The two-component PhoR-PhoP system controls both primary metabolism and secondary metabolite biosynthesis in *Streptomyces lividans*. Proc. Natl. Acad. Sci. U. S. A. **100:**6133–6138.
46. **Sola-Landa, A., A. Rodríguez-García, E. Franco-Domínguez, and J. F. Martín.** 2005. Binding of PhoP to promoters of phosphate-regulated genes in *Streptomyces coelicolor*: identification of PHO boxes. Mol. Microbiol. **56:** 1373–1385.
47. **Sola-Landa, A., A. Rodríguez-García, A. K. Apel, and J. F. Martín.** 2008. Target genes and structure of the direct repeats in the DNA-binding sequences of the response regulator PhoP in *Streptomyces coelicolor*. Nucleic Acids Res. **36:**1358–1368.
48. **Strohl, W. R.** 1992. Compilation and analysis of DNA sequences associated with apparent streptomycete promoters. Nucleic Acids Res. **20:**961–974.
49. **Tanaka, A., Y. Tacaño, Y. Ohnishi, and S. Horinouchi.** 2007. AfsR recruits RNA polymerase to the *afsS* promoter: a model for transcriptional activation by SARPs. J. Mol. Biol. **369:**322–333.
50. **Toulokhonov, I. I., I. Shulgina, and V. J. Hernandez.** 2001. Binding of the transcription effector ppGpp to *Escherichia coli* RNA polymerase is allosteric, modular, and occurs near the N terminus of the β′-subunit. J. Biol. Chem. **276:**1220–1225.